Modeling of switching phenomena in phase change memory (PCM) devices

Daniele Ielmini

DEI, Politecnico di Milano, piazza L. da Vinci 32, 20133 Milano – Italy. E-mail: ielmini@elet.polimi.it

ABSTRACT

This work presents recent progresses in the physical modeling of threshold and memory switching in phase-change memory (PCM) devices. Threshold switching will be discussed in terms of a conduction instability due to energy gain of hopping carriers and field redistribution in the amorphous chalcogenide region. A numerical model able to account for the thickness, temperature and material dependence of the threshold voltage and current will be shown. The concluding remarks will aim at elucidating the intimate relationship between threshold and memory switching.

Key words: phase change memory, threshold switching, memory switching, hopping.

1. INTRODUCTION

Phase-change memory (PCM) is believed to become soon a real competitor in the non volatile memory arena [1]. The storage concept in a PCM relies on threshold and phase switching of specific chalcogenide glasses, e.g. $Ge_2Sb_2Te_5$ [2]. Threshold switching consists of a sudden change of conductivity observed in many chalcogenide glasses [3-6] and other amorphous semiconductors (amorphous B, NiO) [7]. Phase (or memory) switching is instead a phase-transition process (from amorphous to crystalline phase and vice versa) allowing for non volatile bit writing in the memory. The physical understanding of both threshold and memory switching is essential for numerical/compact modeling, design and efficient scaling of PCM devices.
Here the recent progress on the physical understanding and modeling of threshold and memory switching is reviewed [8-10]. Threshold switching is described as the result of carrier energy gain in the hopping transport at high electric fields. A numerical model is shown, able to evaluate the profiles of carrier energy and electric field along the chalcogenide layer and the resulting I-V characteristic of memory cells, for different chalcogenide thickness, temperature and mobility gap. Finally, the correlation between threshold and memory switching properties of different phase change materials will be discussed in the light of the newly proposed model for electrical conduction and switching.

2. ELECTRICAL CONDUCTION AT EQUILIBRIUM

Fig. 1 shows the measured I-V characteristic for a PCM device in a reset state, that is prepared in a partially amorphous phase by a proper programming pulse [2]. The cell was fabricated in a 180 nm technology with $Ge_2Sb_2Te_5$ (GST) as active material, and has a contact area of about 1000 nm^2 and a chalcogenide thickness of about 90 nm [11]. The I-V curve displays three distinctive regions: at low current, a *subthreshold* region, where the current increases with voltage according to a linear behavior (for $I < 5x10^{-8}$ A in Fig. 1) or to an exponential behavior (for $I > 5x10^{-8}$ A in Fig. 1). At a threshold current of about $I = 2x10^{-6}$ A, *threshold switching* is seen, corresponding to an abrupt decrease of voltage for increasing current.

The conduction in the subthreshold regime was interpreted as due to thermally-assisted hopping of carriers among localized states in the disordered structure of the amorphous chalcogenide [8-10]. The concentration of localized states is significant in an amorphous material: localized states can result from point defects (e.g. dangling bonds, vacancies, etc.) and, more generally, from chemical and bond disorder. Anderson demonstrated in fact that a non-periodic potential generally leads to localized states for electrons and holes [12,13]. Due to this large concentration of traps, acting as donor and acceptor levels, the Fermi level is located at a deep energy in the mobility gap, typically around midgap. Trapped electrons/holes can receive energy from thermal fluctuations, thus eventually reaching sufficient

energy to efficiently tunnel toward a new localized state, or even drift in delocalized (free-carrier) states in the conduction or valence band, before they relax their excess energy again and become trapped at deep energy close to the Fermi level.

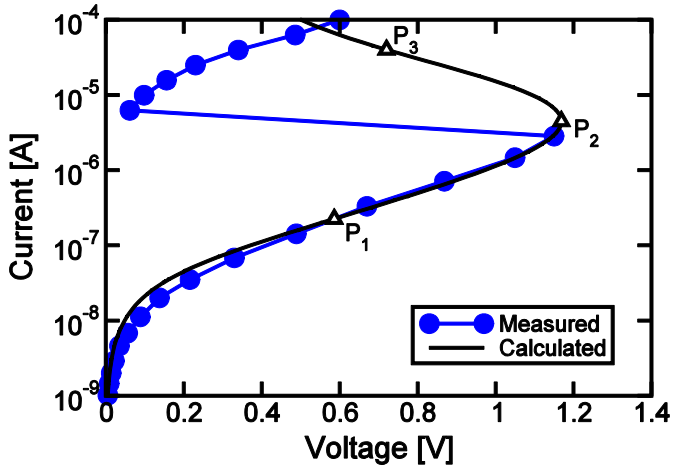

Fig. 1 Measured and calculated I-V characteristics for a PCM device in the reset state, i.e. partially amorphous phase of the active chalcogenide material. The subthreshold regime, threshold switching and ON state can be seen.

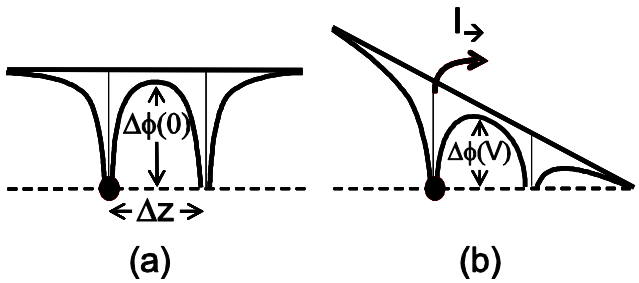

Fig. 2 Schematic for the thermally-activated hopping transport in the amorphous chalcogenide. For hopping between two localized states located at a distance Δz, a trapped electron has to overcome a potential barrier Δϕ(0) at zero electric field (a). Under an applied voltage, the barrier is lowered thus enhancing the transport in the direction of the electrostatic force (b).

A reasonable physical picture for electron hopping between two donor states located at a distance Δz from each other is shown in Fig. 2: when no voltage is applied (V=0, Fig. 2a), the electron sees a potential barrier of height Δϕ(0), and the average escape time τ_e toward the new trap is given by:

$$\tau_e=\tau_0\exp\left(\frac{\Delta\phi(0)}{kT}\right)=\tau_0\exp\left(\frac{E_C'-E_T}{kT}\right), \quad (1)$$

where τ_0 is the characteristic time constant for the electron attempt to escape ($\tau_0 = 10^{-14}$-10^{-13} s for thermally activated hopping [13]), k is the Boltzmann constant, T is the temperature, and Δϕ(0) is given by E'_C-E_T, that is the difference between the conduction mobility edge E'_C and the trap level E_T [8,9]. In Eq. (1), two conduction mechanisms are merged together, namely (1) thermally-assisted tunneling, whereby an electron is raised at a high energy below the top of the potential barrier and then tunnels through the barrier, and (2) Poole-Frenkel emission, where the electron directly hops to the conduction band and freely drifts to the next state [10]. These two mechanisms were shown to have similar magnitude and similar voltage and temperature dependence, thus the simplified Eq. (1) can efficiently describe both effects. Under an applied voltage V (Fig. 2b), the potential barrier is proportional to the square root of the voltage for Δz >> 5 nm (i.e. relatively small trap density), as expected from the standard Poole-Frenkel theory [9].

For $\Delta z << 5$ nm, i.e. for relatively large trap densities, the potential barrier lowering is approximately given by $qV\Delta z/2u_a$, where u_a is the amorphous chalcogenide thickness [9]. The emission time thus reads:

$$\tau_e=\tau_0\exp\left(\frac{\Delta\phi(V)}{kT}\right)=\tau_0\exp\left(\frac{E_C'-E_T}{kT}\right)\exp\left(-\frac{qV}{kT}\frac{\Delta z}{2u_a}\right), \quad (2)$$

while the corresponding current density J is obtained integrating hopping contributions at different E_T, thus yielding:

$$J=2qN_T\frac{\Delta z}{\tau_0}\exp\left(-\frac{E_C'-E_{F0}}{kT}\right)\sinh\left(\frac{qF\Delta z}{2kT}\right), \quad (3)$$

where N_T is the trap density in the upper half of the mobility gap, E_{F0} is the equilibrium Fermi level and $F=V/u_a$ is the electric field [9]. The sinh function in Eq. (3) results from the composition of forward and reverse hopping currents at low electric field [9]. The model in Eq. (3) was demonstrated to account for (i) the shape of the I-V curve in Fig. 1, (ii) the T dependence of the current, (iii) the voltage dependence of the activation energy in the linear and exponential regimes, (iv) the T dependence of the subthreshold slope and (v) the correlation between resistance and subthreshold slope [8,9].

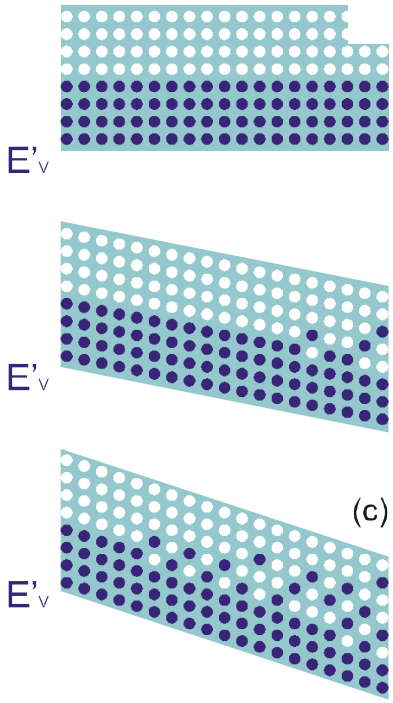

Fig. 3 Schematic for the carrier energy gain at high electric field. (a) equilibrium transport, (b) negligible energy gain $E_F-E_{F0} << kT$ at low fields and (c) off-equilibrium transport with high average excess energy ≈ kT.

3. CARRIER ENERGY GAIN AND THRESHOLD SWITCHING MODEL

The model for electrical conduction in Eq. (3) is strictly valid only at equilibrium, i.e. at relatively low electric field. For relatively high electric field, electrons and holes can gain significant excess energy thus affecting their hopping speed. Fig. 3 shows a schematic for the transition from equilibrium to off-equilibrium, where the electron effective temperature becomes significantly higher than the lattice temperature. In Fig. 3a, electrons and holes obey to the Fermi distribution with an equilibrium E_{F0} under zero applied voltage. When an electric field is applied, carriers start to gain energy by the electric field, similarly to hot carriers in crystalline semiconductors, e.g. silicon in a MOS transistor at high drain voltage. The energy-gain process can be described by the quasi-Fermi level E_F, that is the

energy level for which the distribution function is ½. E_F replaces E_{F0} in Eq. (3) for a general description of transport under off-equilibrium conditions. An *average excess energy* can be correspondingly defined as E_F-E_{F0}. For a moderate electric field, the energy gain by electrons and holes is small, namely E_F-E_{F0} << kT, thus affecting negligibly the current density in Eq. (3). For high electric fields, the energy gain can reach a value close to kT, which corresponds to a current enhancement by a factor *e* in Eq. (3). This carrier energy gain can result in a collapse of the local electric field, thus leading to a negative-differential-resistance (NDR) conduction regime in the I-V characteristic [9,10].

The average excess energy of electrons can be estimated considering the energy gain and relaxation contributions of trapped carriers. The rate of energy gain can be given by:

$$\left.\frac{dE_F}{dt}\right|_{gain} = qFv = \frac{FJ}{n_T}, \tag{4}$$

where v is the average hopping velocity and n_T is the density of trapped carriers contributing to the current. The trapped carrier density can be obtained integrating the exponentially-decreasing distribution function in the upper half of the mobility gap, thus yielding $n_T = N_T kT/(E'_C-E_{F0})$. The rate for energy relaxation can be given by [15]:

$$\left.\frac{dE_F}{dt}\right|_{loss} = -\frac{E_F-E_{F0}}{\tau_{rel}}, \tag{5}$$

where τ_{rel} is the characteristic time for energy relaxation by electron-phonon interaction [10,13,15]. The energy balance for the flux J/q [$cm^{-2}s^{-1}$] of hopping electrons in a slice of length dz along the amorphous chalcogenide layer can thus be written as:

$$\frac{JE_F(z+dz)}{q} = \frac{JE_F(z)}{q} + \left(\left.\frac{dE_F}{dt}\right|_{gain} + \left.\frac{dE_F}{dt}\right|_{loss} \right) n_T dz, \tag{6}$$

where the left hand side is the energy output at z+dz in [$Jcm^{-2}s^{-1}$], while the right hand side includes the energy input at z and the energy gain and loss within dz. Note that E_F is referred to a reference energy level (e.g. E'_C, E_{F0} or E'_V) in Eq. (6). Expressing the gain and loss rates by Eqs. (4) and (5) respectively, one can obtain the quasi Fermi derivative in space as:

$$\frac{dE_F}{dz} = qF - \frac{qn_T}{J}\frac{E_F - E_{F0}}{\tau_{rel}}, \tag{7}$$

where the first and second terms in the right hand side represent gain and relaxation, respectively.

4. SIMULATION RESULTS

Solving Eq. (7) together with the current-field relationship Eq. (3) and with the field-potential relationship $qF = dE'_C/dz$ allows the calculation of (i) the profiles of E'_C, E'_V, E_{F0}, E_F and F along the chalcogenide thickness for any given current density J and (ii) the overall current-voltage (I-V) characteristic of the device. The calculated I-V curve for a PCM cell is shown in Fig. 1. The thickness of the chalcogenide thickness was assumed u_a = 40 nm, i.e. about half of the available chalcogenide thickness in the cell. The calculated I-V curve is in good agreement with the sub-threshold regime of the measured characteristic, accounting for the transition from ohmic to exponential behavior at about I = 50 nA. Other parameters controlling the subthreshold current were fixed as follows: Δz = 7 nm, E_C'-E_{F0} = 0.3 eV and $N_T = 3x10^{19}$ cm^{-3}. As the switching point is approached, a super-exponential increase of the current is seen, which is also well represented by the model. Above the switching point, the calculated curve displays an NDR region, whereas experiments just show a sudden drop of the voltage to about 50 mV. To explain this strong difference, one should consider that, when the switching point is reached in the cell, the high conductivity ON state is established within a switching time $\tau_S \approx 0.1$ ns [3]. The transition to the ON state occurs first at constant voltage due to the presence of a parasitic capacitance C = 12 pF in our experimental set up [16]. Then, since a fixed-current

measurement procedure was used to collect data in Fig. 1, the measurement equipment (HP4155B Semiconductor Parameter Analyzer) actively readjust the voltage to establish a low current (I ≈ 5 μA at the switching point). The voltage readjustment may however take several μs, thus allowing sufficient time for complete crystallization of the amorphous chalcogenide. As a result, the measured I-V characteristic is not representative of the initial amorphous chalcogenide, and should not be taken as a reference.

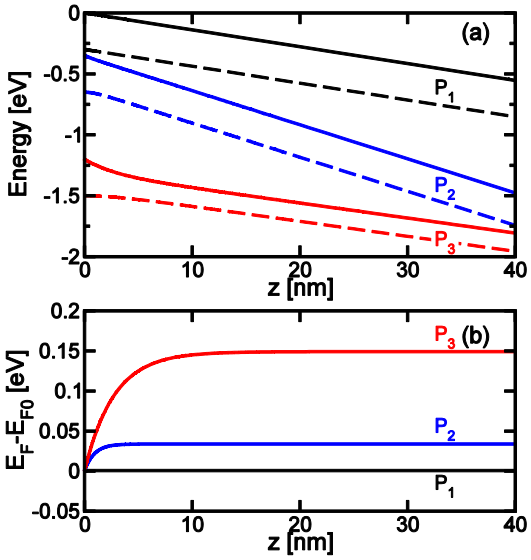

Fig. 4 Calculated profiles of conduction band mobility edge E'_C and quasi Fermi level E_F for bias points P_1, P_2 and P_3 displayed in Fig. 1.

For a more detailed understanding of the switching mechanism in this model, Fig. 4 shows the calculated profiles of E'_C and E_F (a) and of the average excess energy E_F-E_{F0} (b) for the three bias points P_1, P_2 and P_3 shown in Fig. 1. For a low bias current at P_1 (I = 200 nA), the average excess energy is practically zero and the electric field is uniform along the amorphous chalcogenide thickness. At threshold switching (bias point P_2), the excess energy is E_F-E_{F0} = 30 meV, thus slightly higher than kT. This is the result of the field-induced energy gain due to the relatively high energy gain. Note also from Fig. 4b that the excess energy is not uniform, but increases from 0 to a saturated level for small z, close to the cathode. This is because, for low E_F-E_{F0}, the excess energy linearly increases with z, as easily obtained by Eq. (7) for small enough E_F-E_{F0}, where the relaxation term can be neglected [10]. However, due to relaxation, E_F-E_{F0} cannot increase indefinitely and a saturated value can be found at sufficiently large z from Eq. (7) as:

$$E_F - E_{F0} = \frac{FJ\tau_{rel}}{n_T}, \qquad (8)$$

which is proportional to the dissipated power density $P''' = JF$ and to τ_{rel}. The latter was set to $\tau_{rel} = 10^{-13}$ s, in agreement with [10,13,15] and allowing to account for switching voltages and currents in the I-V characteristic. The non uniform quasi-Fermi level results in a strongly non-uniform hopping conductivity, due to the exponential dependence between current and energy in Eq. (3). As a result, to guarantee current continuity along the amorphous chalcogenide thickness, the electric field has to decrease in the so-called 'ON' region with high excess energy far from the cathode interface.

Field non uniformity becomes significant in the ON state above switching (bias point P_3), where a high energy gain can be seen (E_F-E_{F0} = 150 meV in the ON region). Here, the current increase demands an increased electric field in the OFF state (close to the cathode), which results in an increase of average energy E_F-E_{F0}, with a corresponding increase of conductivity and a decrease of electric field in the ON region. As a result, the overall voltage decreases for increasing current above switching, since the field decrease in the ON region, resulting from energy gain, is more important than the field increase in the OFF space. This gives rise to the characteristics NDR, at the origin of threshold switching.

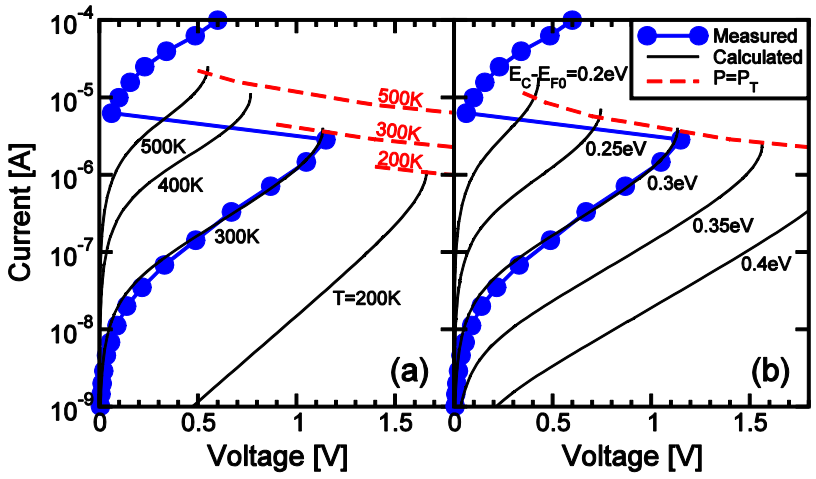

Fig. 5 Calculated I-V curves for increasing temperature (a) and increasing mobility gap (b). Data from Fig. 1 are shown for reference.

Fig. 5a shows calculated I-V curves for increasing temperature. The subthreshold current strongly increases with T due to the thermal activation of the hopping current in Eq. (3), in agreement with experimental results in the literature [8,17]. However, the threshold current I_T only slightly increases. In fact, V_T and I_T are ruled by Eq. (8) and by the condition E_F-$E_{F0} \approx kT$, that is the excess energy at saturation should be at least equal to the thermal energy to trigger the NDR region. This results in a *threshold power* condition which reads $P = FJ = n_T kT/\tau_{rel}$, where the latter term can be identified as a critical power P_T for threshold switching. Curves at constant power $P = P_T(T)$ are shown in Fig. 5, showing that indeed the switching points in the simulations obey to a constant power condition.

Fig. 5b shows calculated I-V curves for increasing mobility gap of the amorphous material. The Fermi level was assumed to be located in the middle of the mobility gap. As a result, an increasing mobility gap dictates an increasing energy barrier for thermally-activated hopping E'_C-E_{F0}, thus resulting in an exponentially decreasing subthreshold current. As also for the T-dependence in Fig. 5a, the threshold current only slightly decreases for increasing gap, since the constant-power locus of switching point appears as a shallow curve on the semi-logarithmic scale in the figure. The threshold voltage V_T decreases for increasing mobility gap: this is because, for increasing mobility gap, the constant P curve intersects the I-V curve at a larger voltage. A similar dependence of V_T on the mobility gap was experimentally observed for stable $(GeTe)_x(Sb_2Te_3)_y$ compounds along the pseudobinary line in [17].

4. THRESHOLD AND MEMORY SWITCHING

Results in Fig. 5b also highlight the intimate relationship between threshold and memory switching in phase change materials. In fact, amorphous semiconductors with a high mobility gap generally displays a high crystallization temperature T_X, thus a high stability under high-temperature bake and a relatively low crystallization speed. For instance, both T_X and the mobility gap increase moving along the pseudobinary line in the GeSbTe ternary diagram from Sb_2Te_3 toward GeTe [18-20]. This should be attributed to the increasing energy difference between bonding (i.e. valence) and antibonding (i.e. conduction) states in the amorphous band diagram. It is this energy difference, in fact, that has to be thermally overcome to locally initiate a transition from the metastable amorphous to the stable crystalline phase. For the sake of completeness, it should be recalled that not only the energy gap, but also the average coordination number <r> contributes to the amount of energy required for thermal initiation of the crystallization process, hence to the crystallization activation energy and crystallization temperature [19,21]. In fact, an increasing number of electrons will have to be excited to the antibonding state for increasing number of bonds in the amorphous structure. The heat of atomization or the cohesive energy, including the effects of both the bonding energy and the amount of structural coordination, has been generally shown to account for crystallization activation energies as a function of chemical composition [21,22].

As a result of the common relationship of crystallization properties (activation energy, crystallization temperature) and mobility gap to the composition-dependent bond energy, the threshold and memory switching display similar

behaviors among different phase change materials. For increasing band gap, a higher V_T (i.e. stability against threshold switching) and a higher T_x (i.e. stability against memory switching) are to be expected. This however should not be seen as a *causal* relationship, but is the result of the similar dependences of threshold and memory switching on the band structure of the amorphous material.

5. CONCLUSION

Recent progresses on the modeling of threshold switching in chalcogenide glasses have been reviewed. Threshold switching is interpreted as due to an energy gain process at high electric fields in the amorphous chalcogenide material. The energy gain results in a collapse of the electric field, leading to a NDR effect and to the threshold switching. The model can account for the temperature and voltage dependence of threshold voltage and current, which are seen to obey a constant power condition. The link between threshold and memory switching is finally discussed.

REFERENCES

1. A. L. Lacaita, "Phase change memories: State-of-the-art, challenges and perspectives", Solid State Electronics 50 (2007) 24.

2. D. Ielmini, A. L. Lacaita, A. Pirovano, F. Pellizzer and R. Bez, "Analysis of phase distribution in phase-change non volatile memories," IEEE Electron Device Lett. 25 (2004) 507.

3. D. Adler, M. S. Shur, M. Silver, and S. R. Ovshinsky, "Threshold switching in chalcogenide-glass thin films," J. Appl. Phys. 51 (1980) 3289.

4. A. Pirovano, A. L. Lacaita, A. Benvenuti, F. Pellizzer and R. Bez, "Electronic switching in phase-change memories," IEEE Trans. Electron Devices 51 (2004) 452.

5. A. Redaelli, A. Pirovano, F. Pellizzer, A. L. Lacaita, D. Ielmini and R. Bez, "Electronic switching effect and phase-change transition in chalcogenide materials," IEEE Electron Device Lett. 25 (2004) 684.

6. D. Ielmini, D. Mantegazza, A. L. Lacaita, A. Pirovano and F. Pellizzer, "Switching and programming dynamics in phase change memory cells," Solid-State Electronics 49 (2005) 1826.

7. H. Fritzsche, "Physics of instabilities in amorphous semiconductors," IBM J. Res. Develop. 13 (1969) 515.

8. D. Ielmini and Y. Zhang, "Evidence for trap-limited transport in the subthreshold conduction regime of chalcogenide glasses," Appl. Phys. Lett. 90 (2007) 192102.

9. D. Ielmini and Y. Zhang, "Analytical model for subthreshold conduction and threshold switching in chalcogenide-based memory devices," J. Appl. Phys. 102 (2007) 054517.

10. D. Ielmini, "Threshold switching mechanism by high-field energy gain in the hopping transport of chalcogenide glasses," Phys. Rev. B 78 (2008) 035308.

11. F. Pellizzer, A. Pirovano, F. Ottogalli, M. Magistretti, M. Scaravaggi, P. Zuliani, M. Tosi, A. Benvenuti, P. Besana, S. Cadeo, T. Marangon, R. Moranti, R. Piva, A. Spandre, R. Zonca, A. Modelli, E. Varesi, T. Lowrey, A. Lacaita, G. Casagrande and R. Bez, "Novel μtrench phase-change memory cell for embedded and stand alone non volatile memory applications," Symp. VLSI Tech. Dig. (2004) 18.

12. P. W. Anderson "Model for the electronic structure of amorphous semiconductors," Phys. Rev. Lett. 34 (1975) 953.

13. N. F. Mott, and E. A. Davis, Electronic processes in non-crystalline materials, (Clarendon Press, Oxford, 1979).

14. D. Ielmini and A. L. Lacaita, "Physical modeling of conduction and switching mechanisms in phase change memory cells," European Phase Change and Ovonics Science Symposium, E/PCOS (2007).

15. A. K. Jonscher, and R. M. Hill, Electrical conduction in disordered nonmetallic films, Physics of thin films, Vol. 8, edited by G. Hass, M. H. Francombe, and R. W. Hoffman (Academic Press, 1975).

16. D. Ielmini, D. Mantegazza, A. L. Lacaita, A. Pirovano and F. Pellizzer, "Parasitic reset in the programming transient of phase change memories," IEEE Electron Device Lett. 26 (2005) 799.

17. X. S. Miao, L. P. Shi, H. K. Lee, J. M. Li, R. Zhao, P. K. Tan, K. G. Lim, H. X. Yang, and T. C. Chong, "Temperature dependence of phase change random access memory cell," Jap. J. Appl. Phys. 45 (2006) 3955.

18. A. L. Lacaita and D. Ielmini, "Reliability issues and scaling projections for phase change non volatile memories," IEDM Tech. Dig. (2007) 157.

19. J. Bicerano and D. Adler, "Theory of the structures of non-crystalline solids," Pure & Appl. Chem. 59 (1987) 101.

20. N. Yamada, E. Ohno, K. Nishiuchi, N. Akahira and M. Takao, "Rapid-phase transitions of GeTe-Sb_2Te_3 pseudobinary amorphous thin films for an optical disk memory," J. Appl. Phys. 69 (1991) 2849.

21. Z. Whang and Q. Chen, "Structure and some physical properties in relation to average co-ordination number, <r>, in TeX and TeXAs glasses," J. Non-Cryst. Sol. 184 (1995) 177.

22. I. Sharma, S.K. Tripathi and P. B. Barman, "Compositional dependence of the physical properties in a-Ge-Se-In glassy semiconductor," Physica B 403 (2008) 624.

Biography

Daniele Ielmini was born in 1970. He received the Laurea (cum laude) and the Ph. D. degrees in Nuclear Engineering from the Politecnico di Milano, Milano, Italy in 1995 and 1999, respectively. In 1999, he joined the Dipartimento di Elettronica e Informazione, Politecnico di Milano, where he became an Assistant Professor in 2002. In 2006 he was a Visiting Scientist at Intel Co., Santa Clara and the Center for Integrated Systems (CIS), Stanford University, Stanford, USA. He has been working on characterization and modeling of CMOS reliability, Flash memories and emerging non volatile memories, such as nanocrystal memories, nitride-trap memories, chalcogenide-based phase-change memories (PCM) and resistive-switching memories (RRAM). He is author/coauthor of more than 100 papers published in international journals and presented in international conferences, and of 3 patents in the field of non volatile memories. He is a member of the Institute of Electrical and Electronics Engineers (IEEE) and of the Material Research Society (MRS). He is a member of technical committees for international conferences such as IEDM (2008), IRPS (2006-2008) and SISC (2008). He received the Impressive Award at E/PCOS 2007.